

## Understanding viscous magnetization of multidomain magnetite

Wyn Williams<sup>1</sup> and Adrian R. Muxworthy<sup>1,2</sup>

Received 15 February 2005; revised 26 August 2005; accepted 25 November 2005; published 18 February 2006.

[1] Viscous magnetization (VM) and viscous remanent magnetization (VRM) have been measured, as a function of temperature, between room temperature and the Curie temperature using a suite of well-characterized synthetic and natural multidomain (MD) magnetite samples. Particular attention was given to possible diffusion aftereffects such as dislocation creep (stress relaxation) and disaccommodation (vacancy and ionic reordering) and their contribution to viscous behavior in what has been commonly thought of as a purely thermal fluctuation process. Dislocation creep was examined by measuring viscosity before and after annealing. Annealing was found to reduce the non- $\log(t)$  behavior, where  $t$  is time. Non- $\log(t)$  behavior has been associated with diffusion aftereffects, suggesting that these are a major contributor to viscosity and (de)magnetization processes in MD samples. The positive curvature of the non- $\log(t)$  acquisition processes indicates that dislocation creep dominates over disaccommodation. This does not imply that VM and VRM are due solely to dislocation creep, but rather that VRM and VM reflect a number of unrelated temperature-dependent processes, primarily thermal fluctuations and dislocation creep. This is the first time that dislocation creep has been directly identified as contributing to viscosity at temperature. These findings will have particular implications for paleointensity determinations, as on heating a sample, its dislocation structure may relax, giving rise to demagnetizations not associated with thermal fluctuations. This will lead to incorrect intensity estimates. If no heating is performed on a geological specimen, then it is very likely that laboratory timescale stress relaxation processes will have already occurred in situ.

**Citation:** Williams, W., and A. R. Muxworthy (2006), Understanding viscous magnetization of multidomain magnetite, *J. Geophys. Res.*, *111*, B02102, doi:10.1029/2005JB003695.

### 1. Introduction

[2] On any change of a magnetic field, the magnetization of a ferromagnetic system relaxes its structures toward a new equilibrium state. If the rate of this change is similar to the observation time then it is said to be viscous (also termed magnetic aftereffect). Changes in magnetization can therefore be regarded as being viscous for time periods as small as a few picoseconds for people examining magnetic switching mechanisms, to millions of years or more for geologists examining rock magnetic recordings of the geomagnetic field. Magnetic viscosity is due to two fundamentally different physical processes: In single-domain (SD) or pseudo-single-domain (PSD) grains the magnetization changes by rotation or switching of the whole magnetization within the grain, whereas in larger multidomain (MD) grains it is the ease with which domain walls move that control the observed viscosity. The ability of magnetic systems to acquire new magnetizations, even in weak fields

like that of the Earth, is of interest to paleomagnetists in order to discriminate possible overprinting of the original remanence, and as such viscosity in natural systems has been much studied over the last 50 years.

[3] Assuming no chemical alteration within the sample during the observation period, the two most significant mechanisms responsible for magnetic viscosity in magnetic minerals are thermal fluctuations and diffusion aftereffects. Thermal fluctuation theories predict that, to a first approximation, the magnetization  $M$  is related to time  $t$  by

$$M \propto \log(t). \quad (1)$$

The slope of this curve ( $\partial M/\partial \log(t)$ ) is characteristic of the relaxation spectra and is usually referred to as the viscosity coefficient  $S_A$  or  $S_D$  for the acquisition and decay coefficients respectively, and these coefficients are a function of field and temperature. Where the energy barriers to domain rotation or domain wall motion in a sample are all equal there will be a uniform distribution of relaxation times, and so  $S_A$  and  $S_D$  will be constant with respect to  $t$ . However, real samples contain distributions of relaxation times, so that  $S_A$  and  $S_D$  will not be constant with respect to  $t$ , giving rise to non- $\log(t)$  behavior. Experimentally non- $\log(t)$  is commonly observed [e.g., Brodskaya, 1970;

<sup>1</sup>Institute of Earth Science, University of Edinburgh, Edinburgh, UK.

<sup>2</sup>National Oceanography Centre, School of Ocean and Earth Sciences, University of Southampton, Southampton, UK.

*Halgedahl*, 1993; *Tivey and Johnson*, 1981], and it can be demonstrated that by expedient choice of a relaxation time distribution function, any type of viscosity law can be obtained [*Tropin*, 1970; *Tropin and Stretskul*, 1972].

[4] For SD assemblages, the thermal fluctuation theory of *Walton* [1980], which extended *Néel's* [1949] theory to include grain distributions, has been experimentally shown to accurately describe interacting and noninteracting SD viscous behavior. In contrast, thermal fluctuation models for MD viscous magnetization have been less successful [e.g., *Aver'yanov*, 1967; *Néel*, 1955; *Stacey*, 1963]. A number of different explanations have been suggested that might account for the lack of success of the thermal fluctuation models in MD minerals: (1) *Néel's* [1950] model is too simplistic; it assumes a uniform distribution of particle properties [*Dunlop*, 1973, 1983]; (2) contamination by SD particles [*Belous et al.*, 1972; *Bol'shakov*, 1975; *Dunlop*, 1983]; and (3) diffusion aftereffects are contributing to viscous behavior [*Moskowitz*, 1985; *Tropin et al.*, 1973; *Tropin and Vlasov*, 1966]. It is to this third explanation which we turn our attention in the rest of this paper.

[5] Thermal fluctuation models assume that once a domain wall has reached a local energy minimum (LEM), it will remain there until a sufficiently large thermal fluctuation event occurs for it to jump to a new LEM. These LEM positions are often related to pinning sites in the crystal structure, such as dislocation lines or impurities. However, it is also possible for these pinning localities to move, especially at high temperatures, giving rise to domain wall movement. This type of mechanism for viscous behavior was termed a diffusion aftereffect by *Moskowitz* [1985]. The movement of dislocations is similar to what is termed in rheology variously as dislocation, power law, high temperature or Weertman creep [*Kearey and Vine*, 1990; *Putnis*, 1992; *Weertman*, 1978]. This type of creep increases with temperature ( $\propto e^{T/T_M}$ ) and becomes significant in the range 0.3–0.7  $T/T_M$ , where  $T$  is the temperature and  $T_M$  the melting temperature ( $T_M \sim 1534^\circ\text{C}$  for magnetite). It is this dislocation creep which is commonly removed from samples by “thermal stabilization” [e.g., *Dunlop and Özdemir*, 2000; *Sholpo et al.*, 1991], and achieved by heating a sample above the temperature at which any future experiments are planned. For a magnetite sample, this typically involves heating the sample at  $600^\circ\text{C}$ – $700^\circ\text{C}$  for an hour, so that during future thermoremanent (TRM) experiments there will be no, or very little, additional dislocation movement.

[6] Often confused with the process described above is another diffusion effect termed disaccommodation, which is attributed to diffusive reordering of vacancies and ferrous ions [*Kronmüller et al.*, 1974; *Néel*, 1952]. Disaccommodation processes and the magnetic history of the sample are interwoven since the longer a sample has been in a steady field or zero field before a change in the field the greater the degree of diffusive reordering, and the smaller the viscous magnetization [*Halgedahl*, 1993; *Sholpo*, 1967; *Tivey and Johnson*, 1984]. In general the amount of disaccommodation will increase with the number of vacancies, although there are a number of mechanisms controlling diffusion of the vacancies and ferrous ions in magnetite, which gives rise to a complex temperature dependency [*Höhne et al.*, 1975; *Kronmüller and Walz*, 1980]. However, it should

be possible to discriminate between dislocation creep and disaccommodation since they contribute to viscosity in fundamentally different ways. Dislocation creep causes a change in the preexisting magnetization; that is, there is movement from one LEM state to another. Disaccommodation, on the other hand, causes a resistance to change; it hardens the magnetic structure [*Trukhin*, 1972].

[7] Previous studies of disaccommodation in MD magnetite involved room temperature measurements only, where the amount of disaccommodation was controlled by varying the time that the sample was kept in a zero field environment before acquisition of a viscous magnetization. These studies have suggested that disaccommodation contributes to viscosity along with thermal activation of domain walls, though there are widely differing views on the relative importance of the two mechanisms [cf. *Sholpo et al.*, 1972; *Tropin et al.*, 1973]. Dislocation creep, on the other hand, has not been explicitly investigated in MD magnetite with the exception of *Skovorodkin et al.* [1976], who found that  $S_A$  increased after applying mechanical stress at room temperature. They attributed this to stress relaxation (dislocation creep) enhancement of viscosity. Interestingly, *Brodskaya* [1970] found that  $\gamma$  radiation, which produces vacancies, decreased room temperature  $S_A$ . This decrease was attributed to an increase in disaccommodation.

[8] In this paper we report experimental data which examine several features of MD magnetic viscosity. In particular we examine, for the first time, the contribution of dislocation creep on magnetic viscosity in MD magnetite as a function of temperature. We report a series of high-temperature viscosity experiments made using a suite of samples. In addition to examining dislocation creep and temperature effects, we also consider the importance inducing field, nonlinearity of viscous behavior, magnetic history and grain size.

## 2. Samples and Instrumentation

[9] The results reported in this paper examine viscosity measurements on a range of natural and laboratory samples, measured on a number of different instruments.

### 2.1. Samples

[10] The MD samples studied in this paper are summarized in Table 1. The samples come from four basic origins; three sets of synthetic samples, and a sample of natural origin *PW*(2 mm). The grain sizes studied cover the range from small pseudo-single-domain (PSD) to large MD samples. The three samples 65B, 83B and 95A were grown by the glass-ceramic method [*Worm and Markert*, 1987], and the magnetic properties of these samples have been described elsewhere [e.g., *Halgedahl*, 1998; *Worm et al.*, 1988]. The two samples *H*(15  $\mu\text{m}$ ) and *H*(23  $\mu\text{m}$ ) were produced by hydrothermal recrystallization [*Heider and Bryndzia*, 1987], and samples *W*(7  $\mu\text{m}$ ) and *W*(11  $\mu\text{m}$ ) were obtained from Wright Industries [*Muxworthy et al.*, 2003a, 2005]. All the synthetic samples were near-stoichiometric or stoichiometric magnetite [*Muxworthy et al.*, 2003a; *Williams*, 1986]. Natural sample *PW*(2 mm) was collected from a green schist on the Shetland Isles, UK, and the magnetite crystals extracted. Mössbauer spectroscopy and

**Table 1.** Physical, Chemical, and Magnetic Properties of the Nine Samples<sup>a</sup>

| Sample              | Grain Size, $\mu\text{m}$ | $\mu_0 H_C$ , mT | $\mu_0 H_{CR}$ , <sup>b</sup> mT | $H_{CR}/H_C$ | $M_{RS}/M_S$ <sup>c</sup> | Chemical Description             |
|---------------------|---------------------------|------------------|----------------------------------|--------------|---------------------------|----------------------------------|
| 65B                 | 1.5                       | 15               | ...                              | ...          | 0.14                      | magnetite                        |
| 83B                 | 7.0                       | 3.8              | ...                              | ...          | 0.03                      | magnetite                        |
| 95A                 | 100.0                     | 1.5              | ...                              | ...          | 0.02                      | magnetite                        |
| $H(15 \mu\text{m})$ | 15(3)                     | 1.5              | 23                               | 14           | 0.0010                    | magnetite                        |
| $H(23 \mu\text{m})$ | 23(5)                     | 0.9              | 21                               | 23           | 0.006                     | magnetite                        |
| $W(7 \mu\text{m})$  | 7(3) <sup>d</sup>         | 6.2              | 25                               | 4.0          | 0.07                      | magnetite                        |
| $W(11 \mu\text{m})$ | 11(3) <sup>e</sup>        | 4.5              | 17                               | 3.8          | 0.07                      | magnetite                        |
| $PW(2 \text{ mm})$  | 2000                      | 0.5              | 17                               | 34           | 0.003                     | magnetite plus trace of titanium |

<sup>a</sup>The grain size distributions for samples were determined from scanning electron micrographs, except for sample  $PW(2 \text{ mm})$ . The grain size standard deviations (where known) are shown in parentheses. The chemical composition was determined from Mössbauer, XRD, and magnetic analysis (this study, Muxworthy [1998], and Muxworthy *et al.* [2003a], Williams [1986], and Worm [1986]).

<sup>b</sup> $H_{CR}$  is the remanent coercive force.

<sup>c</sup> $M_{RS}$  is the remanent saturation magnetization and  $M_S$  is the saturation magnetization.

<sup>d</sup>Mean aspect ratio (AR) is 1.0.

<sup>e</sup>Mean AR is 1.8.

X-ray diffraction (XRD) found that  $PW(2 \text{ mm})$  contained traces of titanium [Muxworthy, 1998].

[11] The hysteresis data, in particular the coercive force ( $H_C$ ) values, suggest the hydrothermal samples have much lower concentration of dislocations than the other the samples. Reflected light microscopy observations on a sister samples found no visible impurities and inclusions in samples  $W(7 \mu\text{m})$ ,  $W(11 \mu\text{m})$ ,  $H(15 \mu\text{m})$ ,  $H(23 \mu\text{m})$  and  $PW(2 \text{ mm})$ .

## 2.2. Instrumentation and Sample Preparation

[12] The data for samples 65B, 83B and 95A were collected using a DC gradient SQUID magnetometer [Williams, 1985]. This machine was used to measure in-field viscous acquisition, that is, viscous magnetization (VM), and decay measurements. Results for the viscous behavior of powdered SD assemblages and glass-ceramics samples measured on this instrument have been reported previously [Williams, 1985; Williams and Walton, 1986, 1988]. The gradiometer was encased in a mu metal can which reduced the “zero field” state in the magnetometer to less than  $\sim 400 \text{ nT}$ . The magnetite grains in the glass-ceramic samples 65B, 83B and 95A were essentially “sealed” from possible oxidation by the surrounding matrix.

[13] Measurements were made on samples  $W(7 \mu\text{m})$ ,  $W(11 \mu\text{m})$ ,  $H(15 \mu\text{m})$  and  $H(23 \mu\text{m})$  and the natural sample using two high-temperature magnetometers. These consisted of viscous remanent magnetization (VRM) measurements made on a two-component spinner magnetometer, and VM measurements on a three-component vibrating sample magnetometer (VSM). Both machines had “zero field” environments of  $\sim 100 \text{ nT}$ . For the VRM measurements made on the spinner magnetometer, the samples were dispersed in Omega high-temperature cement ( $\sim 5$ – $10\%$  concentration) and vacuum sealed in quartz capsules. For the VM measurements, the samples were dispersed in Omega high-temperature cement ( $\sim 5$ – $10\%$  concentration) and then embedded in KBr pellets, after which they were coated in the high-temperature cement. It was hoped that this multilayer technique would reduce the likelihood of oxidation on heating in air. The Omega high-temperature cement is thought to be slightly reducing (J. Marvin, personal communication, 2002). The high-field VM measurement samples were dispersed in Omega high-temperature cement and heated in a helium atmosphere.

Finally, the thermal demagnetization spectra of TRM induced in the samples were measured using the two-component spinner magnetometer.

## 3. VM Versus Temperature in Previously Annealed Samples

[14] Figure 1 shows the acquisition and decay of VM in samples 65B, 83B and 95A as a function of time at various temperatures. The measurements were made on a DC gradient SQUID with an acquisition field of  $144 \mu\text{T}$ . Before each set of experiments the samples were heated to  $\sim 530^\circ\text{C}$  in zero field before cooling to room temperature. The viscous data were measured by heating the sample to the set temperature and holding for five minutes. The acquisition data were then collected followed by the decay data. The first data point of the viscous decay observations was collected less than 3 s after switching off the field. This was repeated at successively higher temperatures. Each viscous curve in Figure 1 has been separated from its neighbors for clarity so that the origin on the  $y$  axis for each curve is arbitrary. The measurements were repeated several times on these samples, and the results were found to be repeatable and consistent.

[15] The acquisition and demagnetization curves are similar to those described by Shimizu [1960] and Dunlop [1983]; as the temperature increases the rate of acquisition and decay also increases. Unlike viscosity results for SD grains the behavior for MD grains tends to be more erratic and less smooth [e.g., Dunlop, 1983; Tivey and Johnson, 1984]. The samples had been heated many times before in previous experiments to  $\sim 530^\circ\text{C}$ , so the contribution of dislocation creep to the viscous behavior can be thought to be essentially zero.

[16] Assuming a linear-logarithmic fit of the form given in equation (1), the acquisition and decay coefficients, respectively  $S_{AI}$  (in-field VM data) and  $S_D$ , are plotted as a function of temperature in Figure 2. The  $x$  axis error on each data point is a qualitative estimate of variation in the temperature during measurement, and the  $y$  axis error bar from the error in the least squares fit of  $S_{AI}$  and  $S_D$  as given in equation (1). Before fitting  $S_{AI}$  and  $S_D$  some data reduction was carried out, in that the data were collected linearly in time at the rate of about one data point every 3 s. After the initial 100 s, the collected data were averaged over

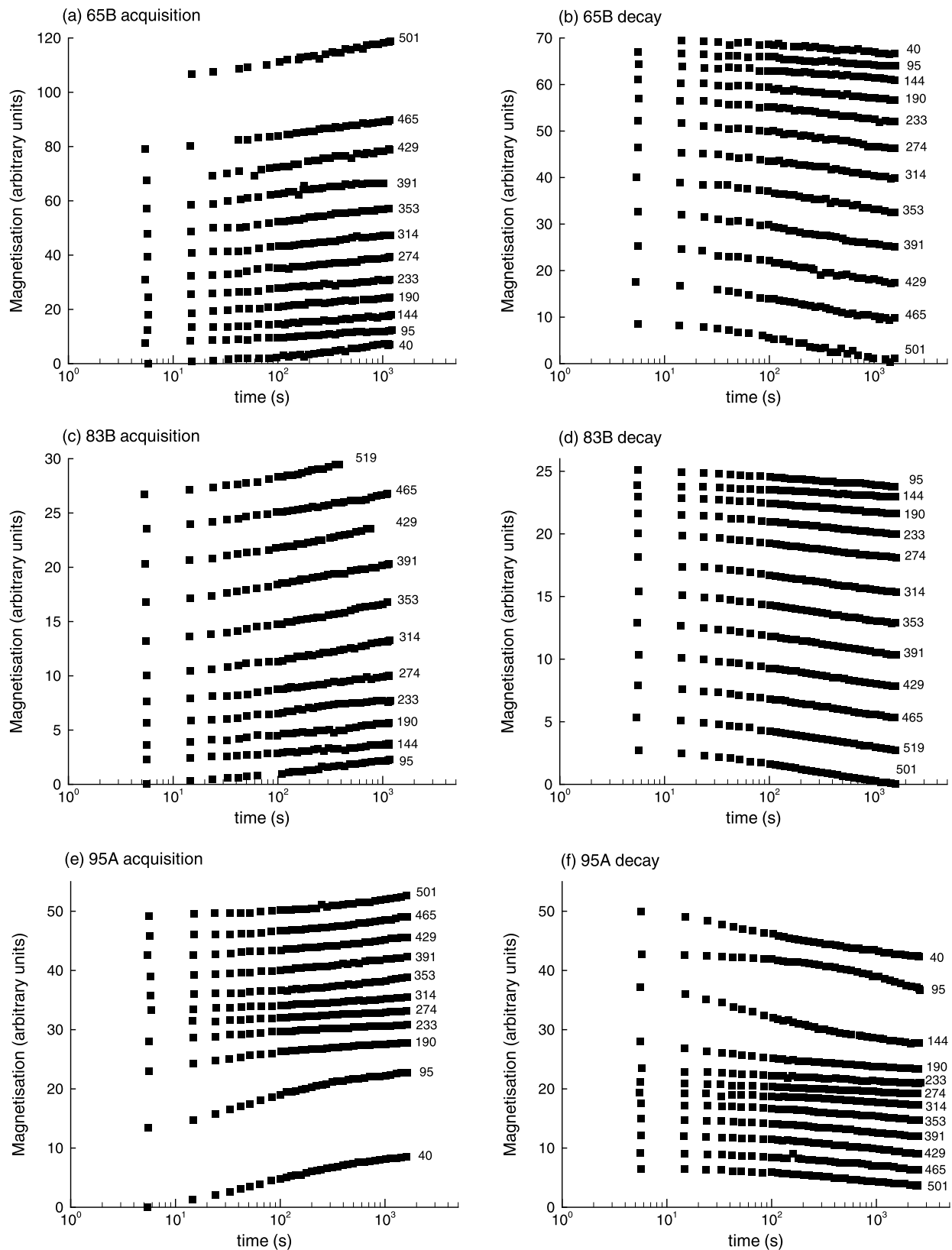


**Figure 1.** VM acquisition and decay curves for samples 65B, 83B, and 95A measured at various temperatures. Initially, the samples were thermally demagnetized, and the data were measured accumulatively. The decay curves on the right follow on from the acquisition curves on the left. The curves have been shifted to remove overlapping and to improve clarity. The inducing field was 144  $\mu$ T.

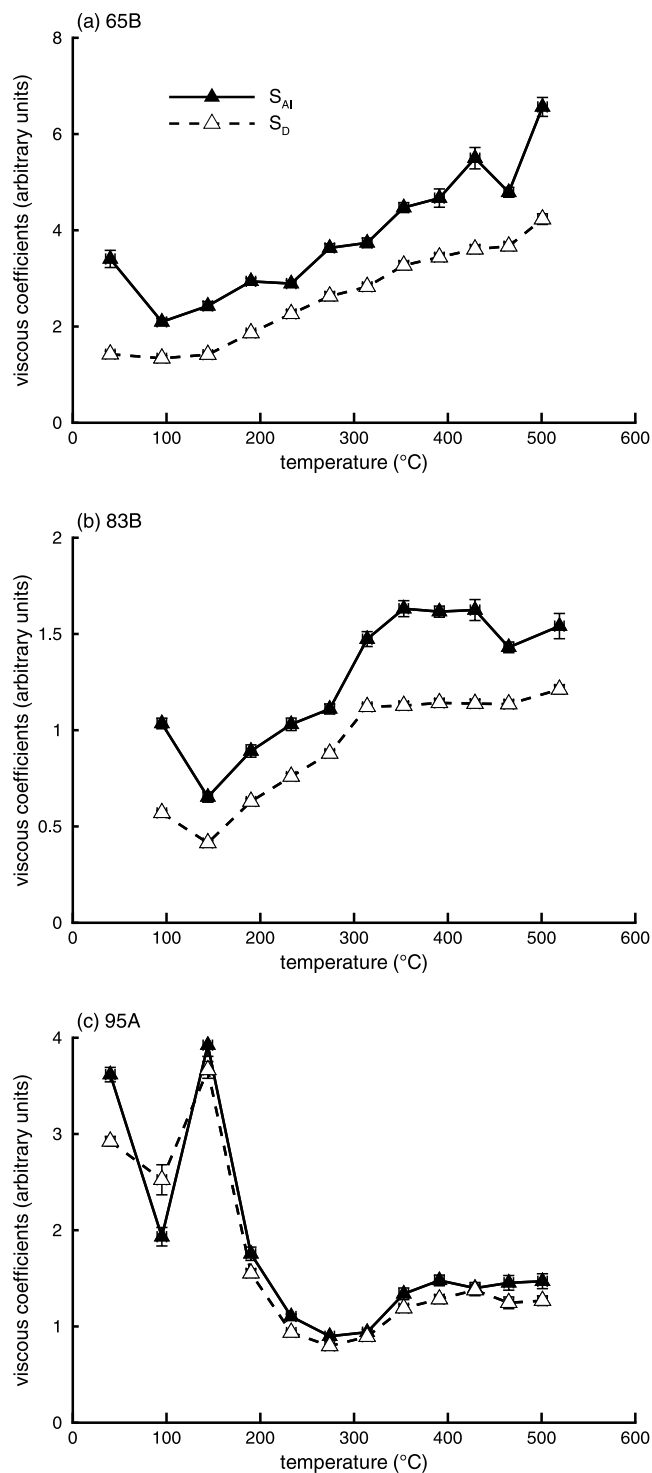


**Figure 2.**  $S_{AI}$  and  $S_D$  versus temperature for samples 65B, 83B, and 95A for VM data. The samples had been previously annealed. The inducing field was  $144 \mu\text{T}$ .  $S_{AI}$  and  $S_D$  were calculated from the corresponding data in Figure 1 using equation (1).

equal increments of  $\log(t)$ , that is,  $\log(t_{i+1}) - \log(t_i) = 0.1$ , where  $t$  is time, and  $i$  the measurement step. To be consistent with other published values of viscosity coefficients, the values reported in this paper were obtained using a least

squares best fit to a  $\log(t)$  function. The nonlogarithmic behavior expressed by a curvature coefficient is considered in section 5.2.

[17] The three samples show a range of trends; for samples 65B and 83B,  $S_{AI}$  and  $S_D$  both generally increase with temperature. While in sample 95A, at low temperatures  $S_{AI}$  and  $S_D$  both decrease with  $T$ , before increasing again as the Curie temperature ( $T_C$ ) is approached. It could be argued that 65B and 83B also display a decrease in  $S_{AI}$  and  $S_D$  with  $T$  at low temperatures, though this is less pronounced. Similar low-temperature peaks and troughs in  $S_{AI}$  and  $S_D$  have been reported previously in the literature for MD magnetite [Shashkanov and Metallova, 1970], though are not always observed [Shimizu, 1960].

#### 4. Effect of Annealing on Viscosity

[18] To examine the role of dislocation creep, we conducted viscosity experiments before and after annealing. That is, the viscosity was measured in a similar manner described in section 3 for unannealed samples, that is, virgin or fresh samples. Once the maximum temperature had been reached in the experiments, the samples were annealed and the viscous behavior remeasured using the same procedure. We examined both VM as well as VRM.

##### 4.1. VM

[19] VM was measured as a function of temperature using an inducing field of  $0.55 \text{ mT}$ . The samples were statically AF demagnetized in three directions at room temperature before each viscosity acquisition and decay measurement. The peak AF field was  $100 \text{ mT}$ .  $S_A$  and  $S_D$  are plotted as a function of temperature for samples  $W(7 \mu\text{m})$  and  $W(11 \mu\text{m})$  in Figure 3 before and after annealing. Generally  $S_{AI}$  and  $S_D$  increase with temperature. It is seen that the effect of annealing is to decrease the viscosity rates  $S_{AI}$  and  $S_D$ . This reduction in  $S_{AI}$  and  $S_D$  is possibly due to dislocation creep; however, it is possible that the reduction is due to chemical alteration rather than dislocation creep, as the samples were only coated in reducing Omega high-temperature cement and heated in air.

##### 4.2. VRM

[20] Previous sections have concentrated on VM, that is, in-field measurements, here we report experiments for VRM. The experiments are essentially the same as the VM measurements, except that the field is switched off during the  $\sim 30 \text{ s}$  period required to measure the magnetic moment. This means that over short time periods VM and VRM data are likely to differ, but over longer periods of time they are expected to be similar. In many respects it is this VRM which is of greater interest to the paleomagnetist, as it is remanent magnetization which is normally measured in the laboratory. The VRM measurements reported here were obtained using an applied field of  $2.0 \text{ mT}$  ( $2000 \mu\text{T}$ ).

[21] For these experiments the samples were vacuum sealed in quartz glass capsules. The samples were initially AF demagnetized in three directions at the beginning of the experiments, though because of the size of the quartz capsules, it was not possible to AF demagnetize during the experimental procedure itself. Therefore, during the viscous experiments the magnetic states were accumulative

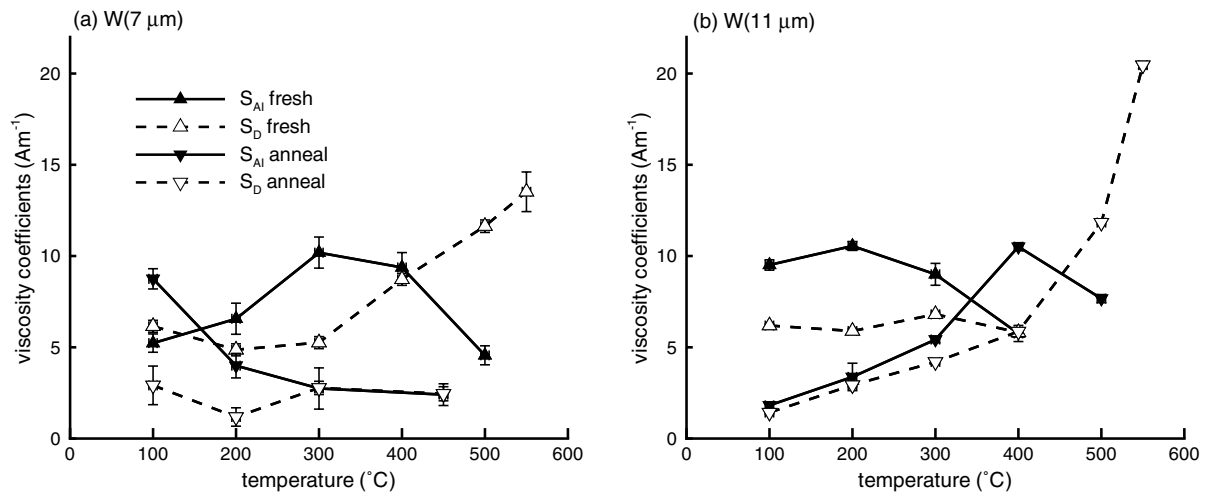


**Figure 3.**  $S_{\text{AI}}$  and  $S_{\text{D}}$  versus temperature for samples  $W(7 \mu\text{m})$  and  $W(11 \mu\text{m})$  for VM data before and after annealing. The samples were AF demagnetized at room temperature between each acquisition and decay measurement. The inducing field was  $550 \mu\text{T}$ .

in a similar manner to section 3; that is, there was no demagnetization between viscosity measurements. This means that the initial state for the “fresh” viscosity measurement (at  $100^{\circ}\text{C}$ ) was AF demagnetized, but the “annealed” measurement at the same temperature was

thermally demagnetized state. The samples were cooled down to room temperature between temperature changes.

[22]  $S_{\text{AR}}$  ( $S_{\text{A}}$  for out-of-field VRM data) and  $S_{\text{D}}$  versus temperature are shown in Figure 4 for samples  $W(11 \mu\text{m})$ ,  $H(15 \mu\text{m})$ ,  $H(23 \mu\text{m})$  and  $PW(2 \text{ mm})$ .  $W(11 \mu\text{m})$  increases

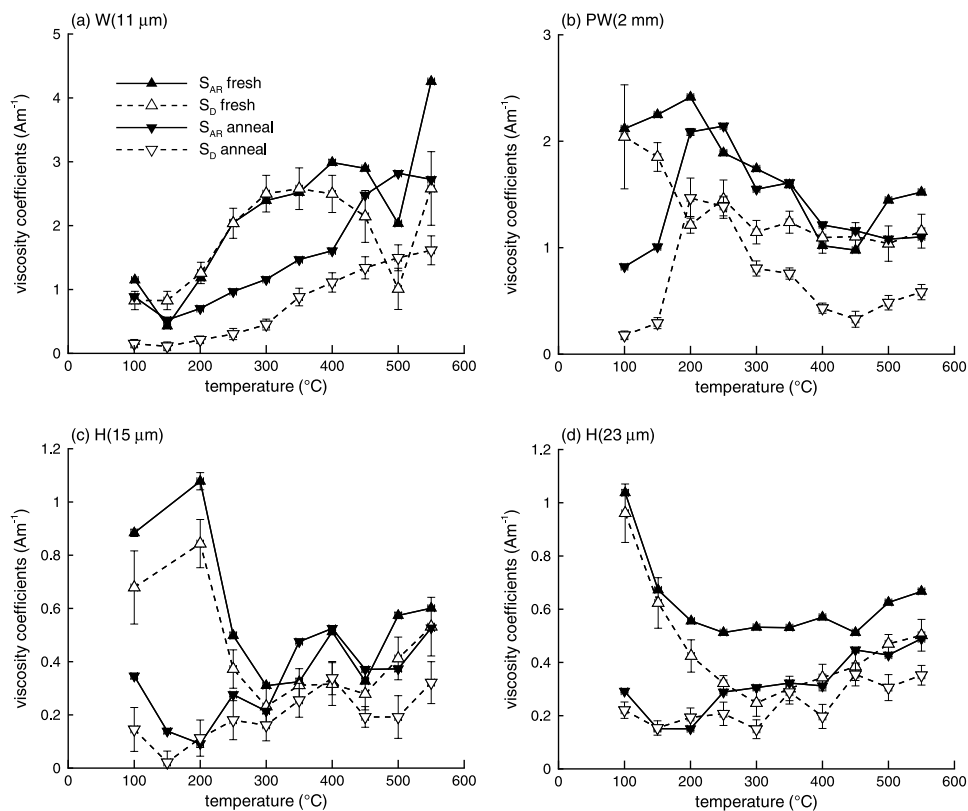


**Figure 4.**  $S_{\text{AR}}$  and  $S_{\text{D}}$  versus temperature for samples  $W(11 \mu\text{m})$ ,  $PW(2 \text{ mm})$ ,  $H(15 \mu\text{m})$ , and  $H(23 \mu\text{m})$  for VRM data before and after annealing. The samples were initially AF demagnetized, and then the viscosity was measured accumulatively. The inducing field was  $2 \text{ mT}$  ( $2000 \mu\text{T}$ ).

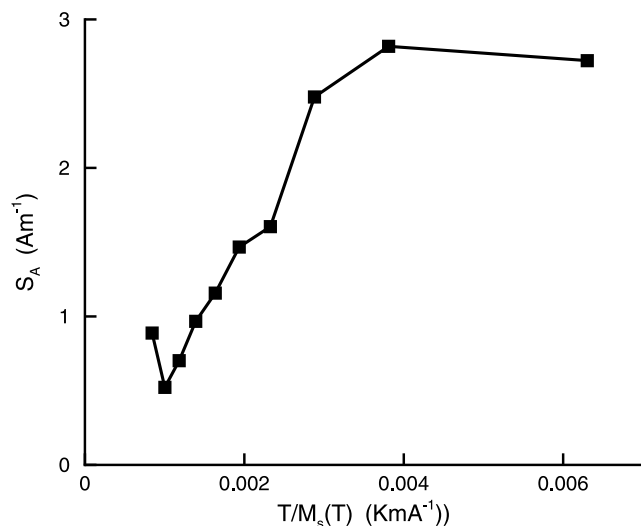


**Figure 5.**  $S_A$  versus  $T/M_S(T)$  for  $W(11 \mu\text{m})$  after annealing. According to equation (2), this plot should yield a straight line. The  $S_A$  data were depicted in Figure 4a.

with temperature, with the peak at  $300^\circ\text{C}$ – $400^\circ\text{C}$  being removed on annealing. The other three samples display more complex behavior.  $S_{AR}$  and  $S_D$  for the fresh  $PW(2 \text{ mm})$  decreases with temperature, while for the annealed data there is a peak in the range  $200^\circ\text{C}$ – $300^\circ\text{C}$ . Both  $H(15 \mu\text{m})$  and  $H(23 \mu\text{m})$  display similar trends; for the “fresh” data  $S_{AR}$  and  $S_D$  decrease sharply with temperature before increasing slightly on approach to  $T_C$ . The absolute values for  $S_{AR}$  and  $S_D$  are significantly higher in samples  $W(11 \mu\text{m})$  and  $PW(2 \text{ mm})$  than in samples  $H(15 \mu\text{m})$  and  $H(23 \mu\text{m})$ .

[23] For both VM and VRM observations, a general decrease in viscosity coefficients is observed after annealing. In our view this can be attributed to dislocation creep in the following way. A movement of dislocations enhances viscosity since it provides an additional mechanism by which domain walls are activated as a function of temperature. Annealing of dislocations essentially removes this contribution, leaving only the thermal activation of domain walls as the source of magnetic viscosity. Since the component of viscosity due to dislocation creep is reduced on annealing, the viscosity coefficients themselves should also be smaller.

## 5. Discussion

[24] There are a limited number of reports which detail the variation of viscosity coefficients for magnetite with temperature [Barbier, 1954; Dunlop, 1983; Shashkanov and Metallova, 1970; Shimizu, 1960; Williams, 1986]. A remarkable feature observed on comparing  $S_A$ ,  $S_D$  vs.  $T$  plots for both SD and MD assemblages, is the deterioration of the uniformity of the curves as the samples’ grain size increases. Generally, these studies report a steady increase in  $S_A$  and  $S_D$  with temperature for SD assemblages, but for MD grains the behavior is more complicated. For PSD and MD assemblages some studies find a systematic increase and others a more irregular increase, occasionally with a low-temperature peak. That the low-temperature peaks are removed or reduced by annealing suggests that the origin of this low-temperature feature is dislocation creep.

[25] All MD thermal fluctuation models’ predict for uniform relaxation times predict

$$S_A, S_D \propto T/M_S(T). \quad (2)$$

MD thermal fluctuation models are readily tested by plotting  $S_A$  annealed versus  $T/M_S(T)$  for the VRM data for sample  $W(11 \mu\text{m})$  (Figure 5). It is clear that  $S_A$  does not vary with temperature as predicted by equation (2). Similar behavior was observed for the other samples.

[26] The ratio  $S_A/S_D$  allows for the comparison of acquisition and decay mechanisms and for direct comparison between different samples independent of their mass of magnetite. Most MD thermal fluctuation theories predict  $S_{AI}/S_D$  and  $S_{AR}/S_D$  should both be equal to one [Richter, 1937; Stacey, 1963; Street and Woolley, 1949]. In contrast, Néel’s [1950] thermal fluctuation model predicts  $S_{AR}/S_D = 1$ , and  $S_{AI}/S_D = 2$ . The factor of two in Néel’s MD theory comes from the expressions for the Rayleigh constants, and not an implicit difference in the acquisition and decay spectra.

[27] That MD thermal fluctuation models predict  $S_{AR}/S_D = 1$  and in some cases  $S_{AI}/S_D = 1$ , appears to be logically inconsistent. This inconsistency is also seen in SD thermal fluctuation models, which all predict  $S_{AI}/S_D = 1$  and  $S_{AR}/S_D = 1$  [Néel, 1949; Richter, 1937; Stacey, 1963; Street and Woolley, 1949]. These models assume that domain walls or SD moments, which have acquired a magnetization in a field in time  $t_a$ , will relax in zero field in the same time  $t_a$ . This cannot be correct, since from a simple consideration of statistics, we know that if a subset of grains from an assemblage acquires a magnetization by thermal stochastic processes in time  $t_a$ , then even if the relaxation process in zero field is identical, the amount of time for this smaller subset of particles to relax and completely demagnetize will be statistically greater than  $t_a$ . This is most easily demonstrated by considering noninteracting SD assemblages, where it is possible to explicitly calculate  $S_{AI}/S_D$  (Appendix A). It is seen that  $S_{AI}/S_D > 1$  and in addition that  $S_{AI}/S_D$  is a function of grain distribution. It would appear therefore that the MD thermal fluctuation models are oversimplified, even without considering the implications of diffusion aftereffects.

[28] In Figures 6 and 7,  $S_{AI}/S_D$  and  $S_{AR}/S_D$  are plotted as a function of temperature for a number of samples. The annealed samples in Figure 6 display significant variation at low temperature, with the smallest grain size sample 65B having the highest ratio. On increasing the temperature there is no clear trend and it is seen that  $1 < S_{AI}/S_D < 2$ , similar to the findings of Dunlop [1983] for submicron magnetites. In contrast  $S_{AR}/S_D$  displays greater variation (Figure 7), particularly for the annealed data set. Most of the  $S_{AR}/S_D$  ratios plot between 1 and 2, except in the annealed data sets for  $W(11 \mu\text{m})$  and  $PW(2 \text{ mm})$ . This difference between the data for the fresh and annealed samples may reflect the different initial states; the fresh data are from an initial AF demagnetized state, whereas the annealed data are for an initial thermally demagnetized state. The difference in initial state is discussed below in section 5.3.

### 5.1. Comparison of TRM Unblocking Spectra With $S_D$ : A Test for Thermal Fluctuations?

[29] If viscosity is a purely thermal fluctuation effect, then the sample’s viscosity and TRM unblocking spectra should

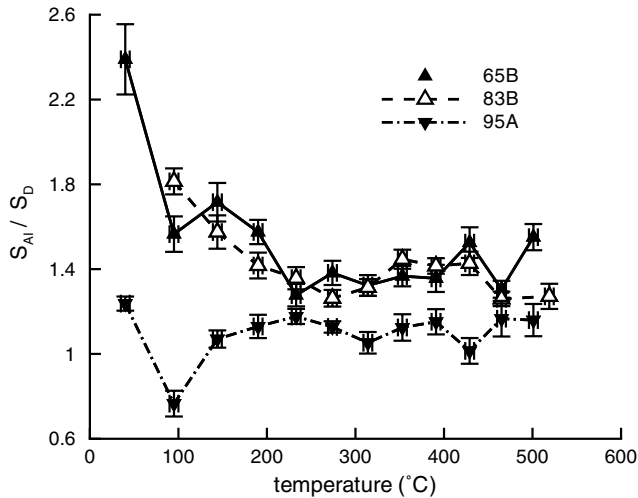


**Figure 6.** Ratio  $S_{AI}/S_D$  temperature for samples 65B, 83B, and 95A.  $S_{AI}$  and  $S_D$  are depicted in Figure 2.

be interrelated. A linear relationship between the two parameters would support the idea that viscosity is due to thermal fluctuations. The TRM unblocking spectrum was determined simply by dividing TRM lost in a particular temperature interval,  $\Delta T$ , by the size of the temperature interval itself. Since TRM is lost more rapidly as the Curie

temperature is approached,  $\Delta T$  was made smaller at higher temperatures. In Figure 8 TRM unblocking spectra (inducing field = 100  $\mu$ T) are plotted against  $S_D$  for the “annealed” data from samples  $W(11 \mu\text{m})$ ,  $PW(2 \text{ mm})$ ,  $H(15 \mu\text{m})$  and  $H(23 \mu\text{m})$ . Only  $W(11 \mu\text{m})$  displays a weak linear correlation between TRM unblocking spectra and  $S_D$ . The other samples all display a large scatter and no clear relationship. This might suggest that the two processes are governed by different mechanisms; that is, viscous behavior is not controlled solely by thermal fluctuations; however, this test is inconclusive for two reasons. First, TRM unblocking spectra represent the average magnetization lost per degree over, say, a 50°C range, whereas  $S_D$  represents the average rate of decrease of an acquired magnetization with time. Therefore, although both parameters in Figure 8 represent demagnetization at or near a given temperature, the exact processes are not identical. Secondly, our poor understanding of the governing processes of MD TRM mean that the lack of linearity between TRM unblocking spectra and  $S_D$  does not provide conclusive evidence for the rejection of the thermal fluctuation of MD viscosity.

**5.2. Non-log(t) Behavior: Evidence for Dislocation Creep?**

[30] It was assumed in sections 3 and 4 that the viscosity varies linearly as  $\log(t)$ . As discussed previously, this is only a first-order approximation and that the behavior is

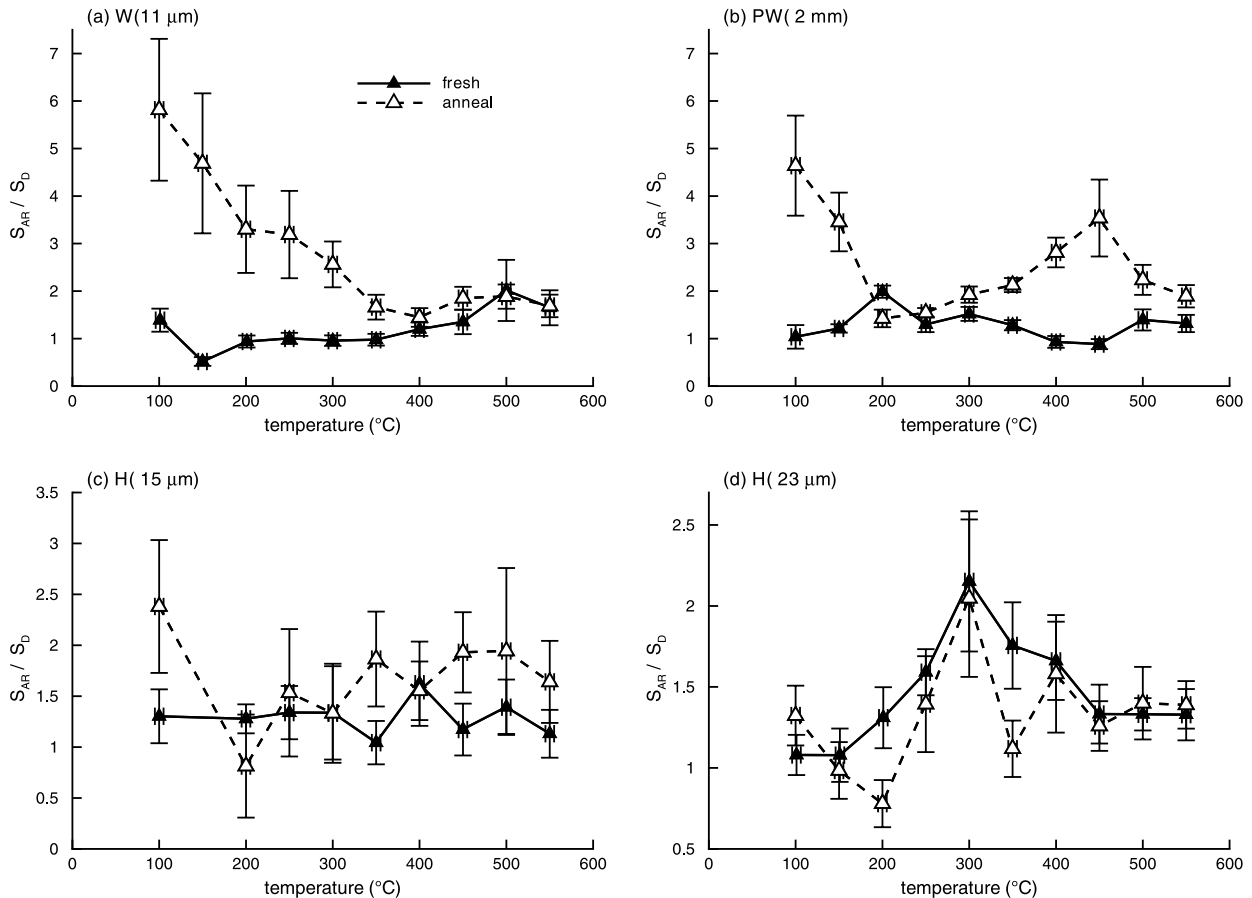


**Figure 7.** Ratio  $S_{AR}/S_D$  temperature for samples  $W(11 \mu\text{m})$ ,  $PW(2 \text{ mm})$ ,  $H(15 \mu\text{m})$ , and  $H(23 \mu\text{m})$  before and after annealing.  $S_{AR}$  and  $S_D$  are depicted in Figure 4.

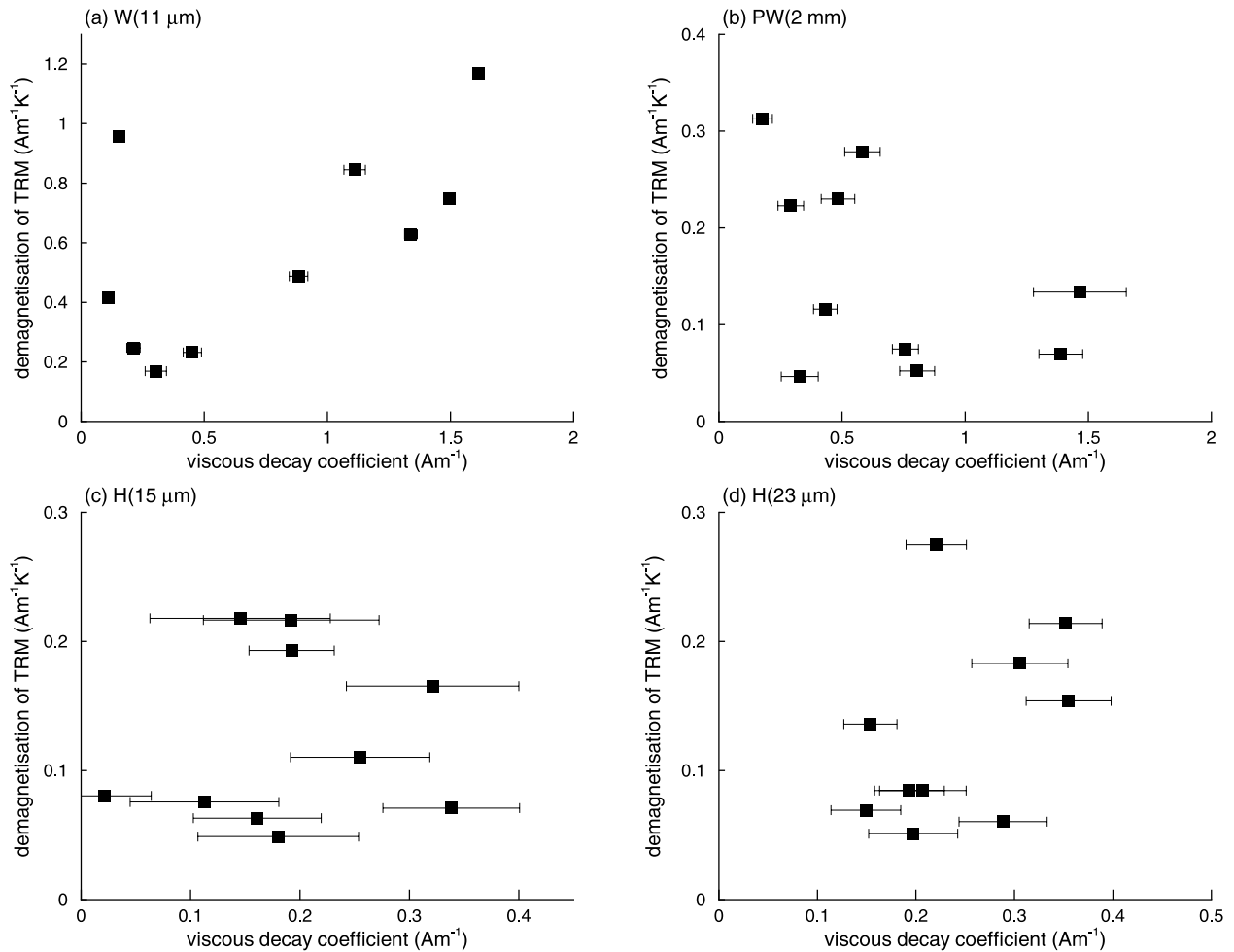


**Figure 8.** Rate of demagnetization of TRM (the TRM lost in any sample per degree Celsius of heating) versus  $S_D$  for samples  $W(11 \mu\text{m})$ ,  $PW(2 \text{ mm})$ ,  $H(15 \mu\text{m})$ , and  $H(23 \mu\text{m})$  after the samples had been annealed.  $S_D$  is shown in Figure 4.

often more complicated; non-log( $t$ ) behavior is commonly observed in both SD and MD assemblages (Figure 9) [e.g., Dunlop, 1983; Trukhin *et al.*, 2003]. Because of our lack of understanding of MD viscous theory, it is difficult to

explain this behavior. However, viscous SD theory predicts such non-log( $t$ ) behavior if magnetostatic interactions and/or grain distributions are included. In many ways interactions between SD moments are analogous to interactions

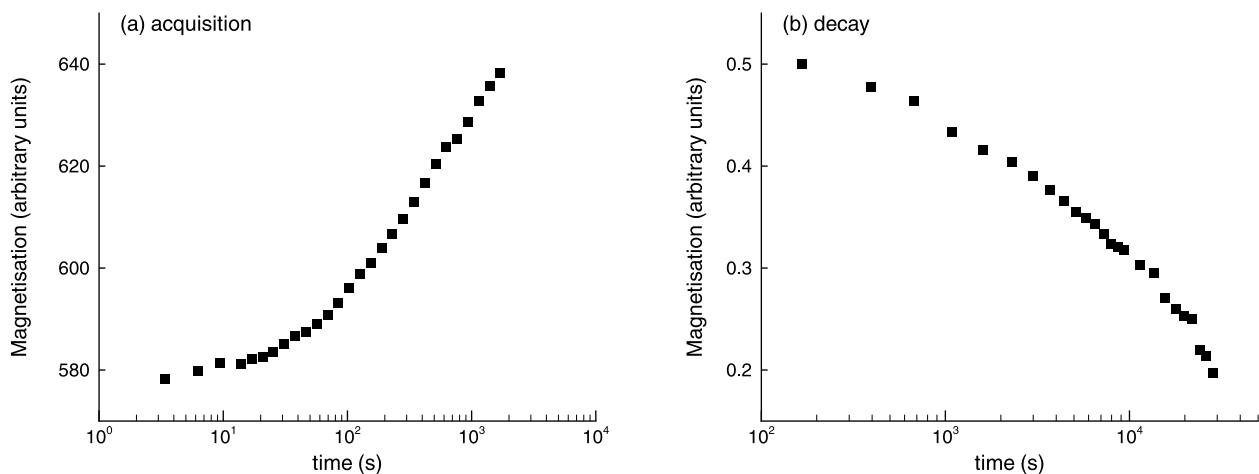


**Figure 9.** (a) VM acquisition curve at  $100^\circ\text{C}$  and (b) VRM decay curve at  $300^\circ\text{C}$  for sample  $W(11 \mu\text{m})$ . Note that the scales have been chosen to enhance the curvature.

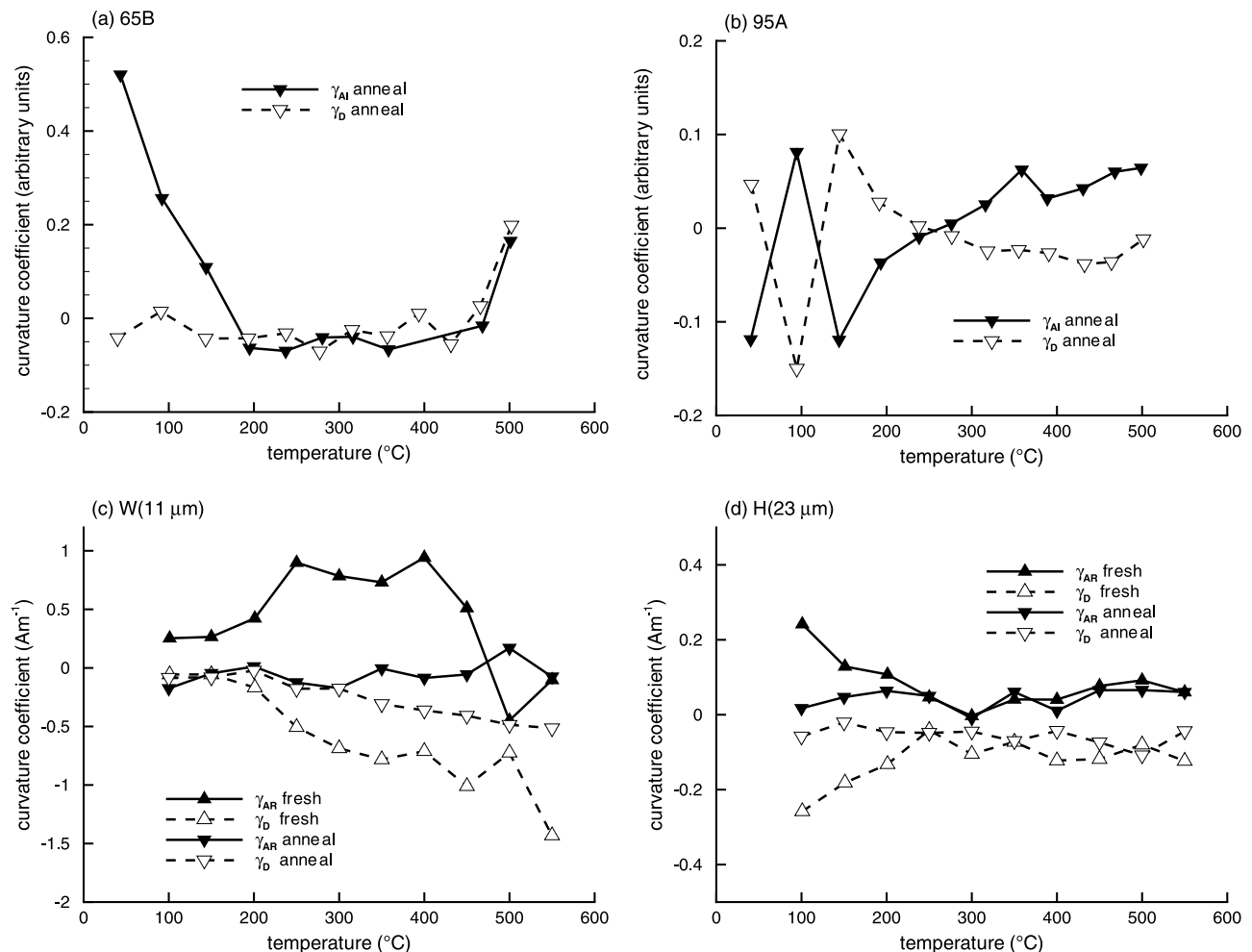


**Figure 10.** Acquisition and curvature parameters  $\gamma_A$  and  $\gamma_D$  versus temperature for the samples 65B, 95A,  $W(11 \mu\text{m})$ , and  $H(23 \mu\text{m})$  before and after annealing. Figures 10a and 10b are for VM data, and Figures 10c and 10d are for VRM data. The curvature parameter is defined in equation (3).

between domains with distributions of domain wall coercivities. It is therefore unsurprising that MD grains display a degree of nonlinear  $\log(t)$  viscous behavior.

[31] To quantify this non- $\log(t)$  behavior it has been common practice to fit a second-order polynomial of the form

$$M = \alpha + \beta \log(t) + \gamma \log(t)^2, \quad (3)$$

where  $\alpha$ ,  $\beta$  and  $\gamma$  are fitted coefficients. For acquisition data where the slopes are positive, an acceleration in the slope as seen in Figure 9a is indicated by a positive curvature parameter  $\gamma_A$ . Similarly, for viscous decay the slope is negative; therefore an increase in the slope as depicted in Figure 9b is indicated by  $\gamma_D$  being negative. In Figure 10,  $\gamma_A$  and  $\gamma_D$  are plotted as a function of temperature for samples 65B, 95A,  $W(11 \mu\text{m})$  and  $H(23 \mu\text{m})$ . Generally, with the exception of 65B,  $\gamma_A$  is positive and  $\gamma_D$  is negative. There is no clear trend with temperature.

[32] On comparison with SD data [Williams, 1986], it appears that there is a gradual shift with grain size, from the truly SD state where  $\gamma_A$  and  $\gamma_D$  are positive, to the truly MD state where  $\gamma_A$  and  $\gamma_D$  are mirrors of each other. Sample

65B falls somewhere in between these two types of behavior (Figure 10a). Since the change in gradient is small and occurs over large time intervals, it is necessary to have good data. For some of the data, especially for the weaker hydrothermally produced sample  $H(23 \mu\text{m})$ ,  $\gamma$  is poorly estimated. The acceleration of both acquisition and decay is not consistent with any published thermal fluctuation theory of MD viscosity, but can be explained by the effects of diffusion aftereffects. Evidence for diffusion aftereffects contributing to the curvature is supported by a reduction in both  $\gamma_A$  and  $\gamma_D$  in the annealed samples, especially in  $W(11 \mu\text{m})$  (Figure 10c).

[33] It should be possible to discriminate between the two diffusion aftereffects of disaccommodation and dislocation creep since they are competing phenomena. Dislocation creep produces higher rates of viscosity at higher temperatures by thermal activation of the movement of dislocations, and this will produce an acceleration of viscosity over that because of thermal fluctuations alone. In contrast, disaccommodation produces a hardening of domain wall locations, making them less likely to move and thus decrease the observed viscosity. As a consequence, if the curvature is due to diffusion aftereffects, and  $\gamma_A$  is positive

and  $\gamma_D$  negative, this suggests that the contribution to the viscosity from dislocation creep dominates over disaccommodation. However, there is a second argument proposed by *Sholpo et al.* [1972], which suggests that it is also possible that disaccommodation processes that occur before viscous acquisition, can produce a similar change in viscosity as that of dislocation creep, that is, making  $\gamma_A$  positive and  $\gamma_D$  negative. *Sholpo et al.* [1972] argue that if diffusion of impurity atoms causes ionic rearrangement to increase domain wall stability, the sample will be left in a state deficient in low-energy domain walls. In terms of the spectrum of domain wall relaxation times, disaccommodation will cause a shift from low to high relaxation times in response to the increase of domain wall stabilities. As a consequence the viscosity coefficient will initially be small because of the lack of low-energy domain walls, but will grow as the observation time approaches the relaxation times of the high energy domain walls. In decay, the reverse process occurs and the slope will increase with the observations time. It is difficult to evaluate the theory of *Sholpo et al.* [1972] in this study, as there was no variation in zero field waiting times to assess disaccommodation. However, as the zero field waiting times in this study were significantly shorter than the viscosity measurement time, the observed nonlinear behavior is more likely due to dislocation creep than to disaccommodation.

[34] In contrast to the majority of our samples, *Trukhin et al.* [2003] found that  $\gamma_D$  measured at room temperature was positive for several mid-ocean basalts bearing MD near-stoichiometric magnetite, suggesting that disaccommodation processes dominate. There are two possible explanations for this difference; first, *Trukhin et al.* [2003] made their measurements at room temperature where the disaccommodation spectra displays a large peak [*Höhne et al.*, 1975], and secondly, if room temperature measurements are made on geological samples, then it is very likely that laboratory timescale stress relaxation processes will have already occurred in situ.

### 5.3. Importance of Initial Starting State

[35] It is thought that the initial magnetic state of the sample is of critical importance to viscosity experiments. However, *Halgedahl* [1993] found that the waiting time before measure a viscosity measurement was far more important than initial state, for example, thermally or AF demagnetized. *Pechnikov* [1967] drew similar conclusions about the initial state. In this study three different initial states were considered; the AF demagnetized state, the thermal demagnetized state (only for room temperature measurements) and the accumulative state. For SD assemblages, this incremental heating should be sufficient to totally remove any viscous magnetization acquired at lower temperatures; however, for MD systems *Dunlop and Özdemir* [2000] have demonstrated that VRM acquired at 200°C in crushed and sized natural crystals of magnetite persists on thermal demagnetization up to  $T_C$ . This goes against classic thermal fluctuation MD theories [*Néel*, 1955], and means that the accumulative state will have a partially magnetized state, compared to the demagnetized states after AF or thermal demagnetization.

[36] The data shown in Figures 2 and 4 are for accumulative initial states, and in Figure 3 for AF demagnetized

initial states. There is arguably a slight difference; in the AF demagnetized data there appears to be a peak in  $S_A$  and  $S_D$  at around 300°C–400°C, and also the absolute values of  $S_A$  and  $S_D$  are higher. The latter difference may be attributed to the different inducing fields and the difference between VM and VRM; however, the former trend is a little more difficult to explain. Previously it was suggested that the peak at 300°–400°C may be a reflection of the coercivity spectrum and/or may be partially due to conversion of maghemite impurities in the samples to hematite. It may also be suggested that this peak is a reflection of the difference between an accumulative state and AF demagnetized state; however, the pattern of behavior does not readily follow any logical argument. It is expected that the AF demagnetized state is in a more demagnetized state than the accumulative state, and that being in a demagnetized state as the temperature increases both  $S_A$  and  $S_D$  would increase more rapidly compared to the accumulative state; that is, domain wall movements would be greater; however, the opposite is observed. Another possibility is that as the accumulative state is further from the demagnetized state and that it has access to more LEMs, which the AF demagnetized state does not. This argument is supported by numerical studies on individual PSD grains [*Muxworthy et al.*, 2003b]. However, this seems an unlikely explanation, because for an assemblage of randomly oriented grains such grain shape, orientation and size-dependent effects important to the numerical model are likely to average out.

## 6. Conclusions

[37] VM and VRM acquisition and decay have been measured in a suite of samples as a function temperature between room temperature and  $T_C$ . By measuring the viscosity before and after annealing, the contribution of dislocation creep (stress relaxation) has been accessed. There is strong experimental evidence to suggest that dislocation creep contributes to the viscous magnetization. Annealing of the sample reduces the nonlinear behavior, and the positive curvature of viscous acquisition suggests that dislocation creep dominates over other diffusion after-effects such as disaccommodation. This the first time that dislocation creep has been directly identified as contributor to viscous behavior. However, it would be incorrect to suggest that dislocation creep is the sole cause of viscosity. After annealing, the samples still displayed significant viscous behavior, suggesting that viscous behavior reflects a number of independent temperature-dependent processes.

[38] If a sample becomes stressed and is subsequently magnetized, then on relaxing the stress of the sample, say, through laboratory heating, this will give rise to “unwanted” changes in the magnetization. This will have implications in particular for paleointensity determinations, as on laboratory heating during a standard paleointensity determination the magnetization will change because of both thermal fluctuations and dislocation creep, giving rise to a false intensity estimates. This change should be detected by paleointensity partial TRM (pTRM) checks, but would be attributed falsely to “chemical alteration.” Directional analysis is less likely to be effected by dislocation creep, though it may give rise to minor deflections of the magnetization in a multicomponent magnetization.

[39] If no heating is performed on a geological specimen, then it is likely that during room temperature measurements, laboratory timescale dislocation-creep processes will have already occurred in situ. Consequently only disaccommodation processes will be observed.

### Appendix A: Viscosity Ratio for Assemblages of Noninteracting SD Grains

[40] The effect of varying grain distribution shape on the magnetic viscosity ratio  $S_A/S_D$  is determined here for SD grains using an extension of *Stephenson* [1971] and *Walton's* [1980, 1983] theories.

[41] The magnetic moment  $M$  of an ensemble of noninteracting SD grains is given by

$$M = \int M_S v n(v) N(v) dv, \quad (\text{A1})$$

where  $M_S$  is the spontaneous magnetization,  $v$  is the grain volume,  $N(v)$  the volume distribution and  $n(v)$  the fractional alignment given by

$$\frac{\partial n}{\partial t} = \frac{(n - n_{eq})}{\tau}, \quad (\text{A2})$$

where  $n$  is the difference between the number of grains aligned with the field minus those aligned antiparallel. The standard expression for the relaxation time  $\tau$  is

$$\frac{1}{\tau} = f_0 \exp\left(-\frac{Kv}{kT}\right), \quad (\text{A3})$$

where  $K$  is the anisotropy and the  $f_0$  atomic rearrangement rate. *Néel* [1949] showed that equilibrium alignment  $n_{eq}$  is given by

$$n_{eq} \simeq \frac{\mu_0 M_S v h}{3kT} \text{ when } h \simeq 0, \quad (\text{A4})$$

where  $h$  is the field,  $k$  Boltzmann's constant and  $T$  temperature. The fractional alignment of domains at any time  $n_t$  will be given by the solution to the ordinary differential of equation (A2). At a constant temperature the following solution can be obtained:

$$n_t = n_0 \exp(-t/\tau) + n_{eq}(1 - \exp(-t/\tau)), \quad (\text{A5})$$

where  $n_0$  is the initial fractional alignment. Then assuming  $N(v)$  varies as  $v^{-r}$  as does *Walton* [1980], defining  $Y = Kv/kT$ , and substituting equations (A3), (A4) and (A5) into (A1), gives for an initially demagnetized state

$$M = \frac{\mu_0 M_S^2 h}{3K} \left(\frac{kT}{K}\right)^{2-r} \int Y^{2-r} (1 - \exp(-f_0 t \exp(-Y))) dY \quad (\text{A6})$$

Because of the observed logarithmic time dependence, the coefficient of magnetic viscosity is defined mathematically as

$$S = \frac{\partial M}{\partial \log(t)} = \frac{\partial M}{\partial t} \frac{\partial t}{\partial \log(t)} = t \frac{\partial M}{\partial t}. \quad (\text{A7})$$

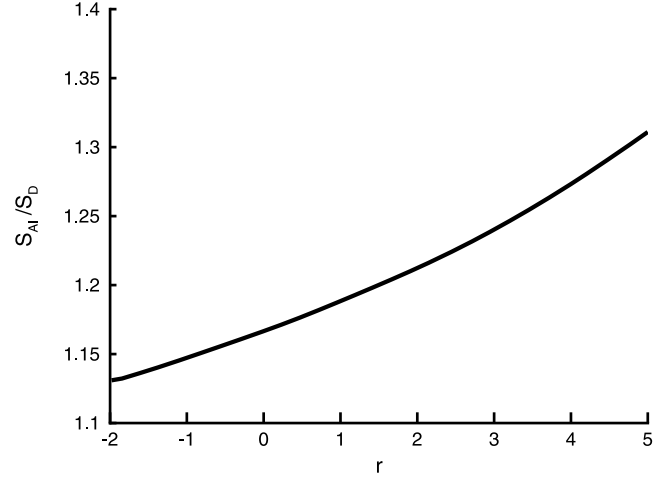


**Figure A1.** Variation of  $S_{A1}/S_D$  versus  $r$  determined numerically using equation (A12). Here  $r$  represents the shape of the grain volume distribution, that is,  $N(v) = v^{-r}$ , for an assemblage of noninteracting SD grains.

Differentiating equation (A6) gives

$$\frac{\partial M}{\partial t} = \frac{\mu_0 M_S^2 h}{3K} \cdot \left(\frac{kT}{K}\right)^{2-r} f_0 \int Y^{2-r} (-\exp(-Y - f_0 t \exp(-Y))) dY. \quad (\text{A8})$$

[42] This can be solved by the method of steepest descents [*Arfken*, 1985] and yields the viscous acquisition coefficient

$$S_{AI} = \frac{C \mu_0 M_S^2 h}{3K} \left(\frac{kT}{K}\right)^{2-r} (\log(f_0 t))^{2-r}, \quad (\text{A9})$$

where  $C$  is a constant. Similarly, the coefficient of viscous decay  $S_D$  may be calculated. The fractional alignment of the sample after sitting in a field  $h$  for  $t_a$  seconds is

$$n = n_0 \exp(-t/\tau) = n_{eq}(1 - \exp(-t_a/\tau)) \exp(-t/\tau), \quad (\text{A10})$$

Following the procedure outlined above, one obtains the following solution:

$$S_D = \frac{C \mu_0 M_S^2 h}{3K} \left(\frac{kT}{K}\right)^{2-r} \cdot \left( (\log(f_0 t))^{2-r} - \frac{(\log(f_0(t+t_a)))^{2-r}}{1+t_a/t} \right). \quad (\text{A11})$$

The ratio of  $S_A/S_D$  is then simply given by

$$\frac{S_{AI}}{S_D} = \left( 1 - \frac{1}{1+t_a/t} \left( \frac{\log(f_0(t+t_a))}{\log(f_0 t)} \right)^{2-r} \right)^{-1} \quad (\text{A12})$$

The ratio  $S_{AI}/S_D$  increases with increasing  $r$ , that is, differing grain distributions (Figure A1).  $S_{AI}/S_D$  was calculated numerically. A typical SD grain distribution is represented by  $r \sim 2$ , with the range  $-2 < r < 5$  representing extreme

limits for  $r$ . Note viscous acquisition  $S_{AI}$  (equation(A9)) is only proportional to  $\log(t)$  for the specific case  $r = 1$ .

[43] **Acknowledgments.** This work was funded through NERC research grant NER/A/S/2001/00539, with additional travel funding from the Royal Society of London and the University of Edinburgh Development Trust. We benefited from the constructive reviews of David Dunlop and an anonymous reviewer. We would like to thank Valera and Valia Shcherbakov for all their help while in Borok. We would like to thank Nic Odling for his help with the hydrothermal recrystallization technique.

## References

- Arfken, G. (1985), *Mathematical Methods for Physicists*, 3rd ed., Elsevier, New York.
- Aver'yanov, V. S. (1967), Contribution to the theory of the thermally activated magnetic viscosity of multidomain particles of ferromagnetic materials 2, *Izv. Russ. Acad. Sci. Phys. Solid Earth*, Engl. Transl., 9, 592–595.
- Barbier, J. C. (1954), Le traînage magnétique de fluctuation, *Ann. Phys.*, 9, 84–140.
- Belous, I. M., et al. (1972), On the thermal activation mechanism of magnetic viscosity in multidomain grains of rocks, *Izv. Russ. Acad. Sci. Phys. Solid Earth*, Engl. Transl., 5, 297–300.
- Bol'shakov, V. A. (1975), On the mechanism of viscous magnetization of rock, *Izv. Russ. Acad. Sci. Phys. Solid Earth*, Engl. Transl., 11, 251–255.
- Brodskaya, S. Y. (1970), Influence of  $\gamma$ -radiation on the process of increase of viscous magnetisation of rocks, *Izv. Russ. Acad. Sci. Phys. Solid Earth*, Engl. Transl., 7, 442–446.
- Dunlop, D. J. (1973), Theory of magnetic viscosity of lunar and terrestrial rocks, *Rev. Geophys.*, 11, 855–901.
- Dunlop, D. J. (1983), Viscous magnetization of 0.04–100 micron magnetites, *Geophys. J. R. Astron. Soc.*, 74, 667–687.
- Dunlop, D. J., and Ö. Özdemir (2000), Effect of grain size and domain state on thermal demagnetization tails, *Geophys. Res. Lett.*, 27, 1311–1314.
- Halgedahl, S. L. (1993), Experiments to investigate the origin of anomalously elevated unblocking temperatures, *J. Geophys. Res.*, 98, 22,443–22,460.
- Halgedahl, S. L. (1998), Revisiting the Lowrie-Fuller test: Alternating field demagnetization characteristics of single-domain through multidomain glass-ceramic magnetite, *Earth Planet. Sci. Lett.*, 160, 257–271.
- Heider, F., and L. T. Bryndzia (1987), Hydrothermal growth of magnetite crystals (1  $\mu$ m to 1 mm), *J. Cryst. Growth*, 84, 50–56.
- Höhne, R., et al. (1975), Magnetic after-effects in titanium-doped magnetite, *Phys. Status Solidi A*, 27, K117–K120.
- Kearey, P., and F. J. Vine (1990), *Global Tectonics*, 302 pp., Blackwell Sci., Malden, Mass.
- Kronmüller, H., and F. Walz (1980), Magnetic after-effects in  $Fe_3O_4$  and vacancy-doped magnetite, *Philos. Mag. B*, 42, 433–452.
- Kronmüller, H., et al. (1974), Magnetic after-effects in magnetite, *Phys. Status Solidi A*, 24, 487–494.
- Moskowitz, B. M. (1985), Magnetic viscosity, diffusion after-effect and disaccommodation in natural and synthetic samples, *Geophys. J. R. Astron. Soc.*, 82, 143–161.
- Muxworthy, A. R. (1998), Stability of magnetic remanence in multidomain magnetite, Ph.D. thesis, Univ. of Oxford, Oxford, U. K.
- Muxworthy, A. R., et al. (2003a), Low-temperature cycling of isothermal and anhysteretic remanence: Microcoercivity and magnetic memory, *Earth Planet. Sci. Lett.*, 205, 173–184.
- Muxworthy, A. R., D. J. Dunlop, and W. Williams (2003b), High-temperature magnetic stability of small magnetite particles, *J. Geophys. Res.*, 108(B5), 2281, doi:10.1029/2002JB002195.
- Muxworthy, A. R., J. G. King, and D. Heslop (2005), Assessing the ability of first-order reversal curve (FORC) diagrams to unravel complex magnetic signals, *J. Geophys. Res.*, 110, B01105, doi:10.1029/2004JB003195.
- Néel, L. (1949), Théorie du traînage magnétique des ferromagnétiques en grains fins avec applications aux terres cuites, *Ann. Geophys.*, 5, 99–136.
- Néel, L. (1950), Théorie du traînage magnétique des substances massives dans le domaine de Rayleigh, *J. Phys. Radium*, 11, 49–61.
- Néel, L. (1952), Théorie du traînage magnétique de diffusion, *J. Phys.*, 13, 249–254.
- Néel, L. (1955), Some theoretical aspects of rock magnetism, *Adv. Phys.*, 4, 191–243.
- Pechnikov, V. S. (1967), On the time variation of magnetic viscosity, *Izv. Russ. Acad. Sci. Phys. Solid Earth*, Engl. Transl., 6, 413–415.
- Putnis, A. (1992), *Introduction to Mineral Sciences*, 457 pp., Cambridge Univ. Press, New York.
- Richter, G. (1937), Über die magnetische Nachwirkung am Carbonyleisen, *Ann. Phys.*, 29, 605–635.
- Shashkanov, V. A., and V. V. Metallova (1970), Temperature dependence of the magnetic viscosity coefficient, *Izv. Russ. Acad. Sci. Phys. Solid Earth*, Engl. Transl., 7, 457–459.
- Shimizu, Y. (1960), Magnetic viscosity of magnetite, *J. Geomagn. Geoelectr.*, 11, 125–138.
- Sholpo, L. Y. (1967), Regularities and methods of study of the magnetic viscosity of rocks, *Izv. Russ. Acad. Sci. Phys. Solid Earth*, Engl. Transl., 6, 390–399.
- Sholpo, L. Y., et al. (1972), Thermally activated nature of the magnetic viscosity of rocks, *Izv. Russ. Acad. Sci. Phys. Solid Earth*, Engl. Transl., 1, 42–46.
- Sholpo, L. Y., V. A. Ivanov, and G. P. Borisova (1991), Thermomagnetic effects of reorganization of domain structure, *Izv. Russ. Acad. Sci. Phys. Solid Earth*, Engl. Transl., 27, 617–623.
- Skovorodkin, Y. P., et al. (1976), Development of viscous remanent magnetization in the presence of mechanical stress, *Izv. Russ. Acad. Sci. Phys. Solid Earth*, Engl. Transl., 11, 476–478.
- Stacey, F. D. (1963), The physical theory of rock magnetism, *Adv. Phys.*, 12, 45–133.
- Stephenson, A. (1971), Single domain grain distributions I. A method for the determination of single domain grain distributions, *Phys. Earth Planet. Inter.*, 4, 353–360.
- Street, R., and J. C. Woolley (1949), A study of magnetic viscosity, *Proc. Phys. Soc. London, Sect. A*, 62, 562–572.
- Tivey, M. A., and H. P. Johnson (1981), Characterization of viscous remanent magnetization in single- and multidomain magnetite grains, *Geophys. Res. Lett.*, 8, 217–220.
- Tivey, M. A., and H. P. Johnson (1984), The characterization of viscous remanent magnetization in large and small magnetite particles, *J. Geophys. Res.*, 89, 543–552.
- Tropin, Y. D. (1970), Use of distribution functions in the analysis of viscous magnetization curves of rocks, *Izv. Russ. Acad. Sci. Phys. Solid Earth*, Engl. Transl., 7, 454–456.
- Tropin, Y. D., and I. A. Stretskul (1972), Distribution function method for study of the magnetic viscosity of rocks, *Izv. Russ. Acad. Sci. Phys. Solid Earth*, Engl. Transl., 8, 566–568.
- Tropin, Y. D., and Y. D. Vlasov (1966), Some aspects of the theory of magnetic viscosity in multidomain rock grains, *Izv. Russ. Acad. Sci. Phys. Solid Earth*, Engl. Transl., 5, 325–328.
- Tropin, Y. D., I. M. Belous, and I. A. Stretskul (1973), On the thermally activated magnetic viscosity of rocks, *Izv. Russ. Acad. Sci. Phys. Solid Earth*, Engl. Transl., 1, 61–62.
- Trukhin, V. I. (1972), Interpretation of data on the magnetic viscosity of rocks, *Izv. Russ. Acad. Sci. Phys. Solid Earth*, Engl. Transl., 4, 235–241.
- Trukhin, V. I., et al. (2003), Magnetic viscosity of basalts from fault zones of the Atlantic Ocean, *Izv. Russ. Acad. Sci. Phys. Solid Earth*, Engl. Transl., 39, 666–675.
- Walton, D. (1980), Time-temperature relations in the magnetisation of assemblies of single domain grains, *Nature*, 286, 245–247.
- Walton, D. (1983), Viscous magnetization, *Nature*, 305, 616–619.
- Weertman, J. (1978), Creep laws for the mantle of the Earth, *Philos. Trans. R. Soc. London, Sect. A*, 288, 9–22.
- Williams, W. (1985), Viscous magnetization of single domain grains, *Geophys. J. R. Astron. Soc.*, 81, 326–327.
- Williams, W. (1986), The effect of time temperature on magnetic remanence, Ph.D. thesis, Univ. of Cambridge, Cambridge, U. K.
- Williams, W., and D. Walton (1986), Demagnetisation of viscous moments, *Geophys. J. R. Astron. Soc.*, 85, 453–459.
- Williams, W., and D. Walton (1988), Thermal cleaning of viscous magnetic moments, *Geophys. Res. Lett.*, 15, 1089–1092.
- Worm, H.-U. (1986), Herstellung und magnetische Eigenschaften kleiner Titanomagnetit-Ausscheidungen in Silikaten, Ph.D. dissertation, Univ. of Bayreuth, Bayreuth, Germany.
- Worm, H.-U., and H. Markert (1987), The preparation of dispersed titanomagnetite particles by the glass ceramic method, *Phys. Earth Planet. Inter.*, 46, 263–269.
- Worm, H.-U., et al. (1988), Thermal demagnetization of partial thermoremanent magnetization, *J. Geophys. Res.*, 93, 12,196–12,204.

A. R. Muxworthy, National Oceanography Centre, School of Ocean and Earth Sciences, University of Southampton, European Way, Southampton SO14 3ZH, UK. (adrian.muxworthy@gmail.com)

W. Williams, Institute of Earth Science, University of Edinburgh, Kings Buildings, West Mains Road, Edinburgh EH9 3JW, UK.